Cooperative pseudo-Jahn-Teller effect of the $Fe(H_2O)_6^{2+}$ complexes in the sulfate heptahydrates

W. Siebke*
Physikalisches Institut der Universität Erlangen-Nürnberg, D-8520 Erlangen, West Germany

H. Spiering and E. Meissner
Institut für Anorganische und Analytische Chemie, Johannes Gutenberg-Universität, D-6500 Mainz, West Germany

(Received 17 March 1982; revised manuscript received 23 July 1982)

The sulfate heptahydrates $MSO_4 \cdot 7H_2O$ crystallize in two different structures: the monoclinic melanterite (M =Fe,Co,Cu,Cr) and the orthorhombic epsomite (M =Mg,Ni, Zn,Mn). An ^{57}Fe Mössbauer-effect study of the mixed crystals $Fe_xM_{1-x}SO_4 \cdot 7H_2O$ (M =Mg,Ni, Zn,Co) has been performed. The temperature dependence of the quadrupole splittings of various mixed crystals and the magnetically (3 T) perturbed powder spectra of $Fe_xZn_{1-x}SO_4 \cdot 7H_2O$ at 4.2 K clearly show that there is an interaction between the Fe^{2+} ions. The interaction, which is observed above a concentration x_c, increases with increasing x and produces two inequivalent Fe^{2+} sites. The energy-level scheme of the orbital states is the same on both sites. The observed phenomena are explained by the cooperative Jahn-Teller (JT) effect in terms of a two-sublattice model with an antiferromagnetic type of interaction between nearest neighbors. This model strongly supports the hypothesis that the JT energy of the JT ions (Fe,Co,Cu,Cr) stabilizes the monoclinic compared with the orthorhombic structure.

I. INTRODUCTION

The sulfate heptahydrates $MSO_4 \cdot 7H_2O$ crystallize in two different structures that are very similar with respect to their basic arrangement: the monoclinic melanterites (M=Fe,Co,Cu,Cr) with the space group $P2_1/c$ and the orthorhombic epsomites (M=Mg,Ni,Zn,Mn) with the space group $P2_12_12_1$.[1] ($MnSO_4 \cdot 7H_2O$ is dimorphous; the more stable modification is the orthorhombic one.) The elementary cell contains four units of $MSO_4 \cdot 7H_2O$. The crystal is built up out of three different parts: the $M(H_2O)_6^{2+}$ octahedra, the SO_4^{2-} tetrahedra, and single water molecules that are not coordinated to the metal ion.[2,3] The compounds of the same structure are completely miscible. Mixed crystals of monoclinic and orthorhombic compounds show a miscibility gap in the concentration range (x_1,x_2).[4,5] At concentrations $x < x_1$ and $x > x_2$ the mixed crystals are single phased with the structures of the pure compound at $x = 0$ and 1, respectively.

A qualitative base for the understanding of the origin of the two different structures is given by Table I, which contains some properties of the cations M^{2+}. The upper group belongs to the epsomites and the lower one to the melanterites. A size effect of the cations can be excluded to be responsible for the different structures by comparison of the ionic radii: $r(Zn^{2+}) > r(Co^{2+}) > r(Mg^{2+})$. Obviously the orbital degeneracy of the electronic ground states of the octahedral $M(H_2O)_6^{2+}$ complex is strongly correlated to both structures. The cations of the epsomite have orbital singlets and those of the melanterites orbital multiplets. Since the orbital multiplets give rise to Jahn-Teller (JT) distortions, the JT energy seems to stabilize the monoclinic structure rather than the orthorhombic structure.[5]

The numerous experimental investigations concerning the electronic structure of the cations in the sulfate heptahydrates[6] are not suited for a systematic comparison of their results which might support the JT picture. The aim of the presented ^{57}Fe Mössbauer measurements carried out on the binary mixed-crystal systems $Fe_xM_{1-x}SO_4 \cdot 7H_2O$ (M =Mg,Ni,Zn,Co) is to elucidate the role of the JT energy with the formation of the two different structures.

TABLE I. The sulfate heptahydrates $MSO_4 \cdot 7H_2O$ crystallize in two different structures. The correlation between the electronic ground states of the sixfold coordinated cation $M(H_2O)_6^{2+}$ in cubic symmetry and the space group of the lattice is obvious.

		Electronic ground state		
M^{2+}	Space group	Free ion	O_h symmetry	r_{ion} (Å)
Mg	$P2_12_12_1$	^1S	$^1A_{1g}$	0.66
Ni	$P2_12_12_1$	^3F	$^2A_{2g}$	0.69
Zn	$P2_12_12_1$	^1S	$^1A_{1g}$	0.74
Mn	$P2_12_12_1$	^6S	$^6A_{1g}$	0.80
	$(P2_1/c)$			
Co	$P2_1/c$	^4F	$^4T_{1g}$	0.72
Cu	$P2_1/c$	^2D	^2E_g	0.72
Fe	$P2_1/c$	^5D	$^5T_{2g}$	0.74
Cr	$P2_1/c$	^5D	^5E_g	0.89

II. EXPERIMENTAL

The mixed crystals were prepared according to the procedure described in Ref. 5. The saturated aqueous solution of the corresponding components was cooled down quickly from ~340 K to room temperature. A crystalline precipitate was obtained by continuously stirring the supersaturated solution. ^{57}Fe was used for samples with a concentration x less than 0.05. The enriched metallic iron (93 at. % ^{57}Fe) was dissolved in diluted sulfuric acid and added to the second component. Because of the small amounts prepared, the crystals were obtained by slow evaporation of the solvent. The concentration x of the Fe^{2+} ions of the mixed crystals was determined by titration and the crystal structure of several representative samples examined by Debye-Scherrer photographs.

III. EXPERIMENTAL RESULTS AND INTERPRETATION

A. Room-temperature measurements

The results of the Mössbauer-effect measurements at 309 K carried out on the four mixed-crystal systems $Fe_xM_{1-x}SO_4 \cdot 7H_2O$, ($M$ = Mg,Ni,Zn,Co) are shown in Figs. 1(a)–1(d). The linewidth and the quadrupole splitting have been plotted versus the Fe^{2+} concentration x. The dotted vertical lines indicate the limits of the concentrations x_1 and x_2 of the miscibility gap. The miscibility gap does not appear within the Fe-Co system. Within the miscibility gap both the orthorhombic and the monoclinic structures are present, having the concentrations x_1 and x_2. The measured spectra are superpositions of the spectra at x_1 and x_2. Therefore, the values of Γ and ΔE_Q are somehow weighted averages that will not be discussed in the following. The linewidths have been corrected for thickness effects and for the linewidth of the source. Their values must be compared with the natural width of 0.0975 mm s^{-1} plus an apparative broadening of about 0.01–0.02 mm s^{-1}.

1. The isomer shift

The isomer shift δ of all measured samples is the same within the experimental error. The value is $\delta = 1.29 \pm 0.01$ mm s^{-1} relative to α-iron at room temperature. This means that δ is independent of the concentration x, of the type of metal ion (M = Mg,Ni,Zn,Co), and of the structure. This fact may be explained by the assumption that the bonding of the $Fe(H_2O)_6^{2+}$ complex is not affected by the lattice. The changes in the second-order Doppler shifts caused by the different Debye tem-

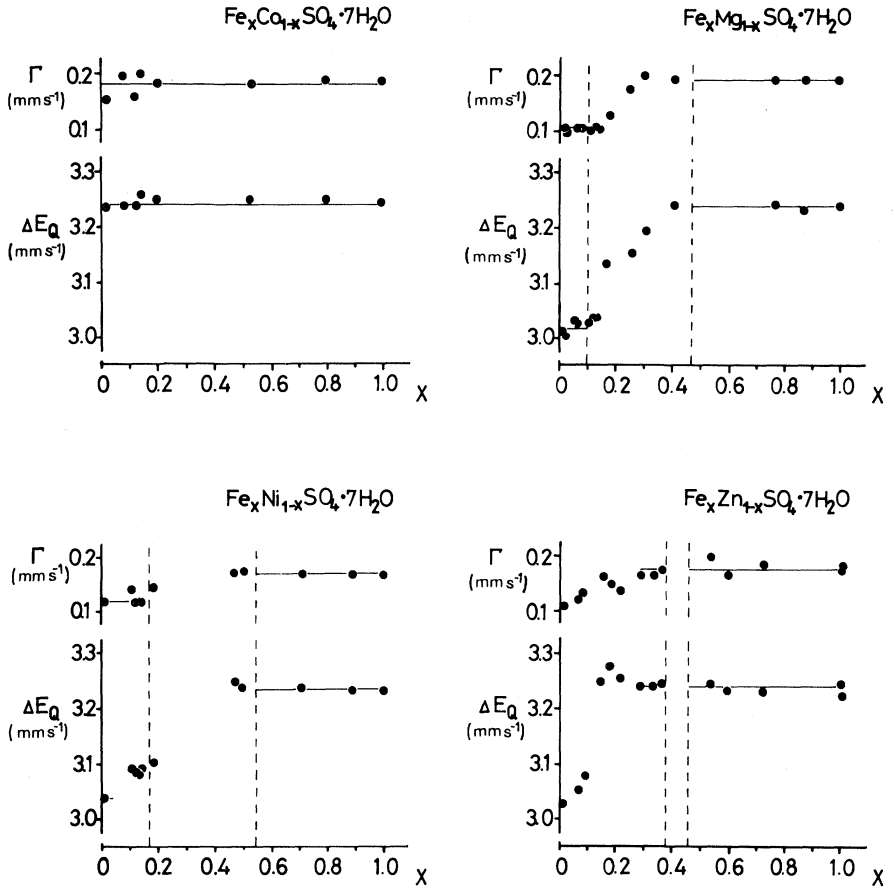

FIG. 1. Linewidth Γ and the quadrupole splitting ΔE_Q plotted as a function of the Fe^{2+} concentration x in $Fe_xM_{1-x}SO_4 \cdot 7H_2O$ where M is Co,Mg,Ni,Zn. The dotted vertical lines indicate the limits of the miscibility gaps. The Fe-Co system is completely miscible.

peratures of the individual structures are too small to be observed.

2. *The quadrupole splitting*

The quadrupole splitting of the isomorphous system $Fe_xCo_{1-x}SO_4 \cdot 7H_2O$ is the same for all mixed crystals ($\Delta E_Q = 3.247 \pm 0.010$ mm s^{-1}), in agreement with the fact that the $Fe(H_2O)_6^{2+}$ complex embedded in the same structure produces the same field gradient at the Fe^{2+} nucleus (Fig. 1). This ΔE_Q value is also found in the mixed crystals $Fe_x(Mg,Ni,Zn)_{1-x}SO_4 \cdot 7H_2O$ on the right-hand side of the miscibility gap ($x > x_2$) where the monoclinic structure is realized. For the same reason the quadrupole splitting of the $Fe(H_2O)_6^{2+}$ complex embedded in the orthorhombic structure of $Fe_x(Mg,Ni,Zn)_{1-x}SO_4 \cdot 7H_2O$ is expected to be the same. This takes place at very low concentrations $x = 0.01$. The differences between the ΔE_Q values are less than 0.020 mm s^{-1}, which is smaller by a factor of 10 than the difference between the values of the orthorhombic and the monoclinic structure (Fig. 1). The situation changes completely if the concentration x increases up to the lower limit of the miscibility gap in $Fe_x(Ni,Zn)_{1-x}SO_4 \cdot 7H_2O$. In the case of $Fe_xZn_{1-x}SO_4 \cdot 7H_2O$ a steep increase of ΔE_Q is observed at $x \approx 0.15$ up to the value of $\Delta E_Q(x = x_1)$, which is the same value as found in the monoclinic structure. For the Ni sulfate heptahydrate the increase of ΔE_Q at $x = x_1$ is much smaller, and for the Mg compound no increase is observed.

We assume now that there is an interaction between the $Fe(H_2O)_6^{2+}$ complexes. This interaction changes the local symmetry of the ferrous complex though preserving the macroscopic symmetry, i.e., the orthorhombic space group of the crystal. The change of the quadrupole splitting as a result of the interaction is different in the Zn and the Ni com-

pound. In the Zn compound the increase of ΔE_Q starts at a concentration around $x=0.08$ and is completed at $x\simeq 0.15$, whereas in the Ni compound the change is already completed at $x\simeq 0.11$. The quadrupole splitting is unaltered in the Mg compound so that the Fe^{2+} ions do not produce a sufficiently large interaction to change their environment in the Mg compound up to a concentration of $x=0.1$, which is the lower limit of the miscibility gap. The measured points within the miscibility gap ($x_1<x<x_2$) are average values of superimposed Mössbauer spectra of mixed crystals belonging to the concentrations x_1 and x_2.

3. *The linewidth*

The different symmetry elements of the monoclinic and orthorhombic structures are responsible for the different linewidths. While the cations of the orthorhombic epsomite occupy general positions, the four $Fe(H_2O)_6^{2+}$ complexes in the unit cell thus being equivalent, the cations of the monoclinic melanterites are located at two special positions that are not related to each other by any symmetry element. Therefore, in the monoclinic lattice there exist two inequivalent Fe^{2+} sites that produce two different quadrupole splittings giving rise to the broadened absorption lines. The fitted quadrupole splittings in Fig. 1 are the average of the splittings caused by the two sites. The mixed crystals of $Fe_xCo_{1-x}SO_4\cdot 7H_2O$ show the broad lines at all concentrations as it is expected from the monoclinic structure. In $Fe_x(Mg,Ni)_{1-x}SO_4\cdot 7H_2O$ below the miscibility gap ($x<x_1$) the linewidths are small corresponding to the equivalence of all sites in the orthorhombic lattice. In $Fe_xZn_{1-x}SO_4\cdot 7H_2O$, however, the situation is quite different and unexpected. At concentrations $x<0.08$ the linewidth is small according to the presence of only one type of lattice site for the Fe^{2+} ions. Around $x=0.15$ the linewidth increases and near x_1 reaches just that value found in the monoclinic lattice. This means that the interaction between the $Fe(H_2O)_6^{2+}$ complexes produces at least two inequivalent sites in the orthorhombic lattice. Remembering the change of the quadrupole splitting at this concentration it becomes very likely that the local environment of the Fe^{2+} ions near x_1 is already the same as in the lattice of ferrous sulfate heptahydrate.

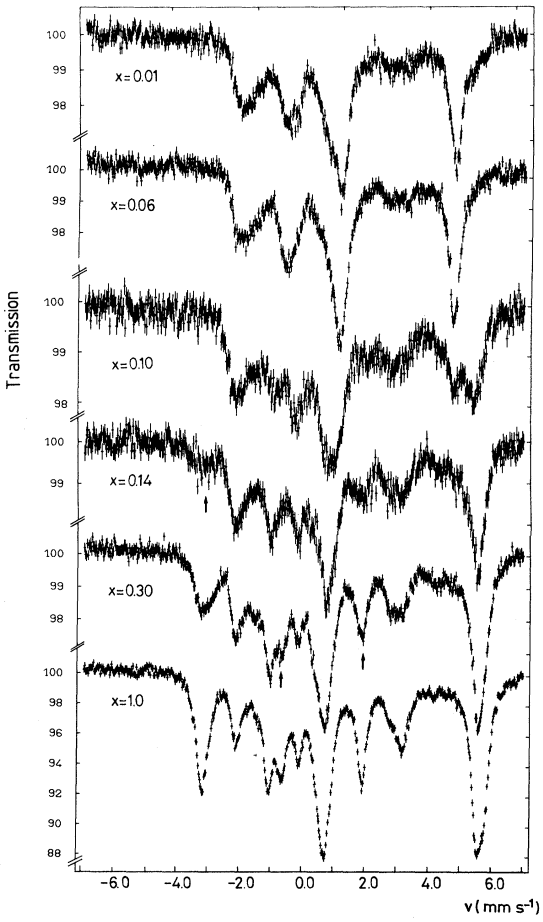

FIG. 2. Powder spectra of $Fe_xZn_{1-x}SO_4\cdot 7H_2O$ measured in a longitudinal magnetic field of 3 T at 4.2 K. Parameter is the concentration x. Three different types of spectra appear with increasing concentration. The arrows mark special absorption lines (see text).

B. Applied magnetic field at 4.2 K

The powder spectra of $Fe_xZn_{1-x}SO_4\cdot 7H_2O$ at 4.2 K perturbed by a longitudinal magnetic field of 3 T are shown in Fig. 2 for different concentrations x. This series of spectra reveal the existence of three different lattice sites. At $x=0.01-0.06$ there is one powder spectrum generated by the isolated Fe^{2+} ion in zinc sulfate heptahydrate. At $x=0.08$ one resolved absorption line appears on the right-hand side of the spectrum. This additional line belongs to a spectrum produced by a second lattice site. At $x=0.10$ both spectra have the same intensity. The other absorption lines of this spectrum more or less overlap with those of the initial spectrum and cannot be identified easily. The third type of spectrum is indicated at $x=0.14$, where at negative velocity (see arrow) a new broad absorption line is formed. The spectrum of the first type has disappeared completely. The intensity of this broad line has increased at $x=0.30$. The two arrows

mark two further lines of the third spectrum. The spectra at $x=0.30$ and the pure ferrous sulfate heptahydrate ($x=1.0$) have almost the same shape. The powder absorption lines become narrower at $x=1.0$, but new lines are not observed. At this stage the following conclusions are evident:

(1) At $0.06<x<0.15$ the interacting Fe^{2+} complexes produce one more spectrum which is different from the spectrum of the isolated complex.

(2) At higher concentrations $0.15<x<x_1$ the spectrum consists of two different spectra that are essentially the same as the spectra of the monoclinic lattice having two inequivalent sites.

Point (2) supports the hypothesis that the cooperative JT effect stabilizes the monoclinic structure. Near x_1 the Fe^{2+} complexes in the orthorhombic lattice arrive at the same shape as the complexes in the monoclinic lattice. The resulting elastic strain energy minus TS_{mix}, where S_{mix} is the mixing entropy, becomes larger than the difference of the free energy between the monoclinic and the orthorhombic lattice.

C. The temperature dependence of the quadrupole splitting

The temperature dependence of the quadrupole splitting ΔE_Q of two examples of the mixed-crystal series is shown in Fig. 3. The decrease of ΔE_Q with increasing temperature T in the range 90 K $<T<$ 310 K strongly depends on the concentration x. The different $\Delta E_Q(T)$ curves result from different ligand fields acting on the $3d$ valence electrons of the Fe^{2+} ions, which are embedded in different environments. The lattice contribution to the electric field gradient (EFG) that mainly originates from the electric dipoles of the water molecules is expected to be small and almost independent of the temperature. This fact is observed in the ^6S state of the Fe^{3+} ion where the $3d$-electron contribution is absent. The ΔE_Q value due to the lattice (ΔE_Q^L) is found to be of the order of 0.5 mm s^{-1} with a decrease of 5% from 4 to 300 K (Ref. 7), which should be compared with $\Delta E_Q(T)$ shown in Fig. 3.

The two inequivalent Fe^{2+} sites of the monoclinic structure show almost the same temperature dependence of the quadrupole splitting, which can be concluded from the linewidth of the superimposed spectra which is nearly independent of tem-

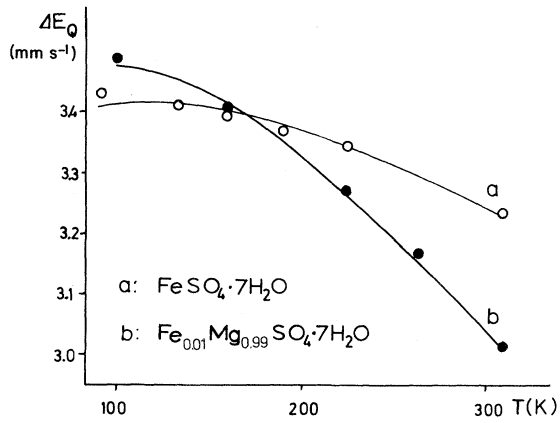

FIG. 3. Quadrupole splitting ΔE_Q of the $Fe(H_2O)_6^{2+}$ complex in the temperature range 90–309 K (curve a) isolated in $MgSO_4\cdot 7H_2O$ and (curve b) in ferrous sulfate heptahydrate decreases with increasing temperature T.

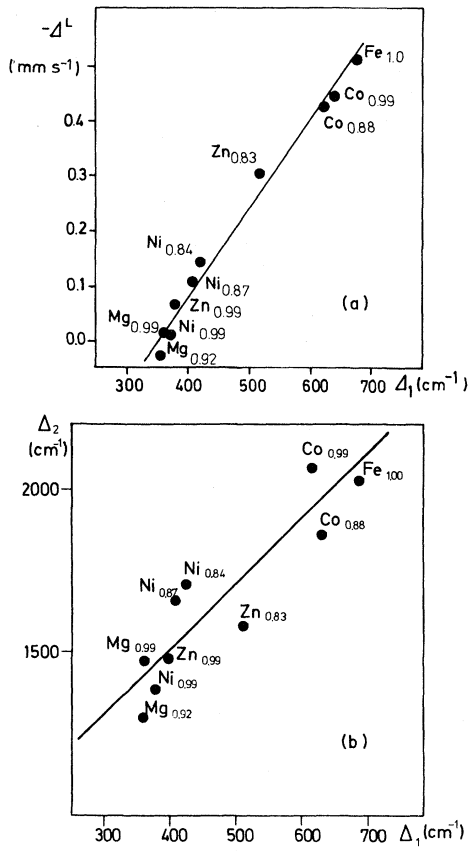

FIG. 4. Ligand-field splittings Δ_1,Δ_2 and the lattice contribution to the quadrupole splitting Δ^L plotted vs each other for different concentrations x of the Fe^{2+} ion of the mixed-crystal series $Fe_xM_{1-x}SO_4\cdot 7H_2O$, M=Mg,Ni,Zn,Co. The points are labeled by M_{1-x}. (a) The negative lattice contribution Δ^L increases linearly with increasing Δ_1 over the whole concentration range x. (b) The large error of Δ_2 is of the order of the deviations from the straight line fitted to the points.

perature. The same holds true for the two ΔE_Q values in the orthorhombic lattice at sufficiently high concentrations of the Fe^{2+} ions where the interaction produces two inequivalent ion sites. Therefore, the average value of $\Delta E_Q(T)$ that differs only by a small amount of about 0.1 mm s^{-1} from the splitting of each site is considered.

The calculation of the ligand-field parameters from the temperature dependence of $\Delta E_Q(T)$ is restricted to the cubic T_{2g} ground state of the Fe^{2+} ion. In D_{2h} symmetry the degeneracy is already completely lifted. The energy levels are described by two splitting parameters Δ_1 and Δ_2 [see Fig. 4(b)]. Two mathematical statements allow the calculation of Δ_1,Δ_2 and of the temperature-independent lattice contribution to the EFG.

The first is given by the fact that the quadrupole splitting due to the T_{2g} valence electrons (ΔE_Q^V) is independent of the special orbital states.[8] Therefore, the orbital states transforming as the irreducible representations of D_{2h} symmetry $\{\varphi_i: xy,xz,yz\}$ can be used for the calculation of ΔE_Q in any symmetry of the ligand field:

$$\Delta E_Q^V=\Delta E_0\,F(\Delta_1,\Delta_2,\lambda,T)\ .$$

The function F (Ref. 9) depends on Δ_1, Δ_2, the effective spin-orbit coupling constant λ, and the temperature T. ΔE_0 is the so-called bare quadrupole splitting of an orbital singlet state ($\lambda=0$, $T=0$). For the $Fe(H_2O)_6^{2+}$ complex the values of ΔE_0 and λ are taken from Ref. 10: $\lambda=-87$ cm^{-1} and $\Delta E_0=4.15$ mm s^{-1}.

There is an interesting consequence for the two inequivalent Fe^{2+} complexes in the monoclinic and the disturbed orthorhombic lattice. From the identical temperature dependencies of $\Delta E_Q(T)$ follows that the energy splittings Δ_1,Δ_2 must be the same. The magnetically perturbed spectra are sensitive to the special orbital states ψ_i, which must be different at least for the ground states of both sites as has been observed in Sec. III B. This degeneracy is discussed in more detail in Sec. IV.

The second statement is proven in Appendix A. The lattice contribution to the electric field gradient is expected to be small enough to use the approximation (A6). With $\Delta E_Q^V=3.2$ mm s^{-1} and $\Delta E_Q^L=0.5$ mm s^{-1} the expansion (A6) is correct within 1%. By neglecting the temperature dependencies of ΔE_Q^L, of the relative orientation of the EFG tensors, and of their asymmetry parameters, the equation

$$\Delta E_Q(T)=\Delta E_0\,F(\Delta_1,\Delta_2,\lambda,T)+\Delta^L$$

determines Δ_1, Δ_2, and Δ^L. Δ^L is proportional to ΔE_Q^L (see Appendix A).

Figures 4(a) and 4(b) show the result of the fits for various concentrations x of the mixed crystals. The estimated error of the Δ_1 values is much less than that of Δ_2 because Δ_2 is much larger compared with kT and λ. Not only a linear relationship between Δ^L and Δ_1 results from the diagrams, but also, and more interesting, the fact that Δ^L and Δ_1 increase with increasing concentration x of the JT ions up to the values of the pure ferrous sulfate. This behavior indicates a cooperative JT interaction between the Fe^{2+} ions (as will be pointed out in Sec. IV). The empirical relationship between Δ^L and Δ_1 is given by $\Delta^L=-1.63\times10^{-3}$ mm s^{-1}/cm^{-1} $\times\Delta_1+0.57$ mm s^{-1}. Additionally, on the basis of the large experimental error for Δ_2, the following proportionality can be given: $\Delta_2=2\Delta_1+750$ cm^{-1}.

IV. DISCUSSION

The ligand-field potential V at the cation site in $(Mg,Ni,Zn)SO_4\cdot7H_2O$ consists of a large cubic part that results from the octahedral coordination of the water molecules and a much smaller low-symmetry part $V(\bar{Q}_i)$. The low-symmetry potential can be expressed by the normal displacements of even symmetry, $\bar{Q}_i$, from the cubic position. This potential causes a splitting of the T_{2g} electron states of the Fe^{2+} ion that substitutes the Mg, Ni, or Zn ion. Off-diagonal elements containing the exited cubic state E_g are assumed to be small compared with the cubic splitting of $\sim10^4$ cm^{-1} between the E_g and T_{2g} state and are not considered here. According to the JT theorem the Fe^{2+} ion tends to change to coodinates Q_i in opposition to the oscillator potential $\frac{1}{2}m\omega_i^2(Q_i-\bar{Q}_i)^2$. The electronic energy gain is caused by the JT matrix element

$$\sum_i\left\langle\varphi_s\left|\frac{\partial V}{\partial Q_i}\right|\varphi_t\right\rangle Q_i=v_{st}\ . \tag{4.1}$$

The $\varphi_s=\{xy,xz,yz\}$ are the T_{2g} electronic states and the $\{Q_i\}=\{Q_u,Q_v;Q_\xi,Q_\eta,Q_\rho\}$ are the normal displacements transforming as the irreducible representations E_g,T_{2g} of the cubic group. In the case of a degenerate T_{2g} state ($\bar{Q}_i=0$) the JT matrix element necessarily splits the orbital state (static approximation). This is the content of the JT theorem. When the $\bar{Q}_i$ are not equal to 0 from the beginning as is known from x-ray studies[3] on the heptahydrate sulfates, the matrix elements v_{st} may nevertheless produce a change. This is called the

pseudo-JT effect (PJTE).

The discussion of the PJTE and the cooperative PJTE, which is believed to explain the observed phenomena, becomes difficult if the complete electronic triplet (T_{2g}) and the five-dimensional (E_g, T_{2g}) displacement space are taken into account. To display the main features the coupling of one displacement with a split electronic doublet is considered in the static JT picture.[1] The Hamiltonian

$$H=\tfrac{1}{2}\hbar\omega q^2+\frac{L}{\sqrt{2}}qS_x+WS_z \tag{4.2}$$

acts upon the pseudospin states $|\pm\rangle$ with $S_z|\pm\rangle=\pm|\pm\rangle$ and $S_x|\pm\rangle=|\mp\rangle$. $q=(m\omega/\hbar)^{1/2}\times(Q-\bar{Q})$ is proportional to the displacement from the equilibrium position. L is the reduced JT coupling matrix element and $\Delta=2W$ the splitting energy of the electronic states caused by the original distortion $\bar{Q}$. The energy potential $H(q,L=0)$ has its minimum at $q=0$ for both electronic states.

There are two additional minima if the characteristic parameter[11] (see Appendix B),

$$S=\frac{L^2}{2W\hbar\omega} \tag{4.3}$$

is larger than 1. These minima appear at the positions

$$\bar{q}_\pm=\pm\frac{\sqrt{2}W}{L}(S^2-1)^{1/2}\,. \tag{4.4}$$

$\bar{q}_\pm$ represents an additional distortion. The energy splitting of the electronic states at $\bar{q}_\pm$ becomes $\Delta=2WS$. The condition (4.3) limits the number of events where a PJT distortion can be expected. Large deviations from cubic symmetry that come from the crystal structure give large energy splittings W and may therefore suppress the JT effect completely.[11] The interaction between the JT molecules is introduced in the molecular-field approximation by the term

$$H_i=-J\bar{q}q\,. \tag{4.5}$$

$\bar{q}$ is the average displacement of the neighboring molecules and J is an interaction constant, which may be positive or negative corresponding to a ferro- or antiferromagnetic type of interaction. Adding (4.5) to (4.2) and minimizing the sum with respect to q produces q as a function of $\bar{q}$. Consistency in the molecular-field approximation in the case $J>0$ requires that $q=\bar{q}$. This condition again results in (4.4) where S is replaced by S':

$$S'=\frac{L^2}{2W(\hbar\omega-J)},\quad S'(J=0)=S\,. \tag{4.6}$$

It is remarkable that even if $S<1$ the value of S' may become larger than 1. In this case the interaction between the molecules leads to an additional distortion by the PJTE. In the molecular-field approximation J is proportional to the number of next neighbors, which can be changed by the concentration x of the JT molecules. The effective interaction constant in the Bragg-Williams approximation is xJ. Therefore, in the case of $S<1$ a critical concentration

$$x_c=\left[\hbar\omega-\frac{L^2}{2W}\right]\Big/J \tag{4.7}$$

can be defined. At this concentration the distortion of the molecule by the PJTE will start. With increasing x the value of $S'=L^2/2W(\hbar\omega-xJ)$ will grow, leading to greater distortions $\bar{q}$ according to (4.4), which determines the lattice contribution Δ^L, and greater splittings of the orbital states $\Delta=2WS'$. To a large extent the described behavior is observed in the Mössbauer spectra of the Ni and Zn compound. At first there is a concentration $x=0.10$, where the change of the ligand-field energies starts; second, the increase of $\Delta_1,\Delta_2,\Delta^L$ with increasing concentration has been found (Fig. 4). The exact situation, of course, is very complicated. A five-dimensional displacement space $\{q_i\}$ must be considered. The interaction between two JT ions that are not equivalent will contain two different displacements q_i^a, q_i^b. In the one-dimensional case the interaction becomes $-Jq^aq^b$. However, the simple relationship between Δ_1 and Δ_2 indicates a simple solution.

The center of gravity of the T_{2g} state remains unchanged by the (T_{2g},E_g) displacements. The equations for the orbital energies

$$E_1+E_2+E_3=0,\quad E_3-E_1=\Delta_2,\quad E_2-E_1=\Delta_1$$

together with the empirical relation $\Delta_2=2\Delta_1+750$ cm^{-1} give the following energies:

$$E_1=-250\text{ cm}^{-1}-\Delta_1\,,$$

$$E_2=-250\text{ cm}^{-1}\,,$$

$$E_3=500\text{ cm}^{-1}+\Delta_1\,.$$

The orbital energy E_2 appears unaffected by the PJTE and a two-state problem is left. This means that the interaction $-Jq^aq^b$ selects such a displacement that only the two electronic levels are concerned. The JT matrix (4.1) belonging to a displace-

ment q with respect to the based states $|\pm\rangle$ has two independent elements $V_{++}=-V_{--}$ and $V_{+-}=V_{-+}$. The diagonal elements V_{ii} do not result in a parameter like S' of (4.6) and in turn demonstrate a critical concentration (4.7). If for simplicity it is assumed that the displacements $q^{a,b}$ transform as the E_g or the T_{2g} representation in cubic symmetry and that they are not of a mixed type, there is only one reduced coupling element $L(E_g)$ or $L(T_{2g})$. At last, to account for the same energy-level scheme of the two inequivalent sites a and b and different orbital states ψ_i^a and ψ_i^b the interaction must be taken antiferromagnetically ($J_a<0$). Then the interaction energy is lowest for $q^a=-q^b$ and the JT off-diagonal matrix elements V_{ij} have opposite signs, $V_{+-}^a=-V_{+-}^b$, but the same absolute values. With $V_{+-}^a=Lq$ and $V_{+-}^b=L(-q)$ we arrive at the simple case discussed above, where J has the value $J=-J_a$ in Eq. (4.6). In opposition to the energy separation $\Delta_2=2WS'$, the eigenstates $\alpha=[(Lq)^2+W^2]^{1/2}$:

$$\psi_1=\frac{1}{\left[2\left[1+\frac{W}{\alpha}\right]\right]^{1/2}}\left[\left[1+\frac{W}{\alpha}\right]\psi_1+\frac{Lq}{2}\psi_3\right],$$

$$\psi_2=\frac{1}{\left[2\left[1+\frac{W}{\alpha}\right]\right]^{1/2}}\left[-\frac{Lq}{\alpha}\psi_1+\left[1+\frac{W}{\alpha}\right]\psi_3\right],$$

depend on the sign of q, which is different for site a and b.

The observation that the environment of the ferrous ion in the Zn compound qualitatively changes in a concentration region ($0.06<x<0.15$) rather than at a critical concentration x_c is easily explained by the invalidity of the Bragg-Williams approximation at low iron concentrations. We assume an additional ferromagnetic type of interaction J_f between equivalent sites (a,a) and (b,b). Then the effective interaction at $x=1$ becomes $J=J_f-J_a$. If the antiferromagnetic type of interaction acts between the two nearest neighbors at a distance of $d=5.924$ Å and J_f between the eight next-nearest neighbors at $d=7.7\pm0.25$ Å the appearance of an additional spectrum (second type) at low concentration $x=0.08$ and the final spectra at $x\simeq0.15$ in Fig. 2 is qualitatively explained by the following arguments. At low concentrations there are a large number of atoms with a next-nearest neighbor and no nearest neighbor, so that the interaction in most cases will be found to be ferromagnetic, leading to the same sign of a distortion q at all sites. The actual sign of q will be determined by higher-order terms $\sim q^3$ in the JT energy. At higher concentration ($x\geq0.1$) the remaining low concentration ($x=0.01$) spectrum does not necessarily originate from isolated complexes. The positive (J_f) and negative interaction (J_a) may add up to a sum less than the critical value J_c [$S'(J_c)=1$] if two nearest neighbors are forced by their different next-nearest neighbors to have the same sign of q. This situation is likely because of the fact that the four equivalent sites in the orthorhombic structure do not form unequivocally sublattices realized in the monoclinic structure. The second lattice site, which appears at $x=0.15$ in Fig. 2, may also be suppressed at low concentrations by this reason. A calculation of the probability of the spectra from a statistical distribution needs the knowledge of the critical value of J_c and the interactions between all sites. Any conclusions from the fraction of the subspectra on the interaction would be very difficult. Nevertheless, an estimation of the upper limit of J and an upper limit of the JT coupling constant L can be obtained from the value Δ_2 at low concentration ($x=0.01$) and of pure ferrous sulfate ($x=1.0$). At $x=0.01$, $S'\leq1$ holds, so that $L^2/2W\hbar\omega\leq1$. Taking $\hbar\omega=250$ cm^{-1} as a typical T_{2g}- and E_g-mode frequency[12] and $\Delta_2=2W$ from Fig. 4(b), the upper limit of L becomes $L\leq600$ cm^{-1}. In $FeSO_4\cdot7H_2O$ the value of $\Delta_2=2.100$ cm^{-1} together with $L=600$ cm^{-1} gives a lower limit for the total interaction of all neighbors: $J\geq80$ cm^{-1}. The values of the JT coupling constants of the $Fe(H_2O)_6^{2+}$ complex have been estimated within the ligand-field approximation.[13] In the notation of Eq. (4.2) the estimated values correspond to $L(E_g,q_\theta)=364$ cm^{-1} and $L(E_g,q_\epsilon)=630$ cm^{-1} or $L(T_{2g},q_i)=932$ cm^{-1}, which compare well with $L=600$ cm^{-1} from above.

A final remark is necessary concerning the minor cooperative effect of the Fe^{2+} ions substituted in the Ni compound and the absence of any effect in the Mg compound. At low concentration $x<0.1$ it has been argued that in the Zn compound the ferromagnetic type of interaction acting between next neighbors produces the distorted environment of the Fe^{2+} ion of the second type. Since the value of the interacting constant J_f depends on the nearest neighbors, which are Mg and Ni hexahydrate complexes that differ in their masses and their vibrational frequencies, the absence of any effect in the Mg compound at $x\leq0.1$ means that the interaction constant is below the critical value necessary for the PJTE. At higher concentration the Mg compound is already becoming unstable, and the monoclinic

compound is formed of a concentration at the higher limit of the miscibility gap x_2. In the Ni compound the increase of the quadrupole splitting up to $x \sim 0.1$ is the same as in the Zn compound and shows no further increase up to the miscibility gap at $x_1 = 0.19$. Here the nearest-neighbor interaction seems to be suppressed. The explanation is very likely given by the larger elastic energy (for the same deformation q) stored in the lattice of the Ni compound as a result of larger elastic constants. From measurements of the velocity of sound[14] the elastic constants are indeed calculated to be 5–10% larger in the Ni compound as compared with the Zn compound.

APPENDIX A

If the quadrupole splitting ΔE_Q results from the superposition of two electric field gradient (EFG) tensors having a different order of magnitude, then the following approximation is useful. The EFG tensor V_{ik}, $i,k=x,y,z$ is the sum of the valence-electron contribution V_{ik}^V and the lattice contribution V_{ik}^L:

$$V_{ik} = V_{ik}^V + V_{ik}^L \ . \tag{A1}$$

The square of the quadrupole splitting

$$\Delta E_Q = \tfrac{1}{2} eQ[V_{zz}^2 + \tfrac{1}{3}(V_{xx} - V_{yy})^2 + \tfrac{4}{3}(V_{xy}^2 + V_{xz}^2 + V_{yz}^2)]^{1/2} \tag{A2}$$

can be written with respect to the principal-axis system S^V of the tensor V_{ik}^V:

$$\Delta E_Q^2 = (\Delta E_Q^V)^2 + (\Delta E_Q^L)^2 + \mathrm{sgn}(V_{zz}^V V_{z'z'}^L)\Delta E_Q^L \Delta E_Q^V f \ , \tag{A3}$$

where $V_{z'z'}^L$ is the tensor component of the lattice contribution with respect to the principal-axis system S^L of the V_{ik}^L tensor. The factor f is a function of the asymmetry parameters η^L, η^V $[\eta = (V_{xx} - V_{yy})/V_{zz}]$ and the Euler angles φ, ϑ, ψ that rotate the system S^L to S^V. Thus,

$$f = \frac{1}{2}\left[\left(1 + \frac{(\eta^L)^2}{3}\right)\left(1 + \frac{(\eta^V)^2}{3}\right)\right]^{-1/2} \left\{3\cos^2\vartheta - 1 - \sin^2\vartheta(\eta^L \cos 2\varphi + \eta^V \cos 2\psi) + \frac{\eta^L \eta^V}{3}[\cos 2\varphi \cos 2\psi(1 + \cos^2\vartheta) - 2\sin 2\varphi \sin 2\psi \cos\vartheta]\right\} . \tag{A4}$$

The absolute value of f is not greater than 1. The quadrupole splitting ΔE_Q, according to Eq. (A2),

$$\Delta E_Q = \Delta E_Q'[1 + (1 - f^2)(\Delta E_Q^L / \Delta E_Q')^2]^{1/2} \tag{A5}$$

is approximately

$$\Delta E_Q' = \Delta E_Q^V + \mathrm{sgn}(V_{zz}^V V_{z'z'}^L)\Delta E_Q^L f \ , \tag{A6}$$

if the condition $(\Delta E_Q^L / \Delta E_Q^V)^2 \ll 1$ is satisfied. Equation (A6) is exact for the special case $|f| = 1$, which means $f = +1$ at $\varphi = \vartheta = \psi = 0°$ and $\eta^V = \eta^L$ or $f = -1$ at $\vartheta = 90°$, $\varphi = \psi = 0°$, and $\eta^V - \eta^L = 1$. If ΔE_Q^L is known to be less than 20% of the measured value, the square root in Eq. (A4) is less than $1 + \frac{1}{2}(0.2)^2 = 1.02$, so that Eq. (A5) is correct within an error of 2%. This situation is met in many cases.

APPENDIX B

The eigenvalues of the Hamiltonian [Eq. (4.2)]

$$H = \tfrac{1}{2}\hbar\omega q^2 + \frac{L}{\sqrt{2}} q S_x + W S_z \ , \tag{B1}$$

are given by

$$E_\pm(q) = \tfrac{1}{2}\hbar\omega q^2 \pm (L^2 q^2/2 + W^2)^{1/2} \ . \tag{B2}$$

If $S = L^2/2W\hbar\omega = 1$, then the minimum energy

$$E_-(\bar{q}) = -\frac{W}{2}\left[S + \frac{1}{S}\right] \leq -W$$

is obtained at $\bar{q} = \pm\sqrt{2}W/L\,(S^2 - 1)^{1/2}$. The electronic energy splitting is $\Delta = 2WS$. If $S < 1$, then the equilibrium position is $\bar{q} = 0$ with an energy separation of $\Delta = 2W$. The interaction $H_i = -J\bar{q}q$ $(J > 0)$ with an average displacement $\bar{q}$ of the neighbors changes the lowest eigenvalue to

$$E_-(q)=\tfrac{1}{2}\hbar\omega q^2-J\bar{q}q-(L^2q^2/2+W^2)^{1/2} . \tag{B3}$$

The condition $q=\bar{q}$ of the molecular-field approximation at the minimum of $E_-(q)$ is obtained replacing $\hbar\omega$ by $\hbar\omega-J$.

The interaction energy of a two-sublattice model with an antiferromagnetic type of interaction ($J_a<0$) between the sublattice a and b and a ferromagnetic one ($J_f>0$) within each sublattice is written as

$$H_i^{\alpha\beta}=-(J_a\bar{q}_\alpha+J_f\bar{q}_\beta)q_\beta,\quad \alpha,\beta=a,b . \tag{B4}$$

The total energy $E_-(\bar{q}_a,\bar{q}_b)$ of the lowest state is the sum $E^a_-(\bar{q}_a,\bar{q}_b)+E^b_-(\bar{q}_a,\bar{q}_b)$, which is given by

$$E_-=\tfrac{1}{2}\hbar\omega q_a^2-(L^2q_a^2/2+W^2)^{1/2}-(J_a\bar{q}_b+J_f\bar{q}_a)q_a+\tfrac{1}{2}\hbar\omega q_b^2-(L^2q_b^2/2+W^2)^{1/2}-(J_a\bar{q}_a+J_f\bar{q}_b)q_b . \tag{B5}$$

The average displacements $\bar{q}_a,\bar{q}_b$ are obtained by the set of equations

$$\frac{\partial E_-}{\partial q_a}=\frac{\partial E_-}{\partial q_b}=0 \tag{B6}$$

and

$$q_a=\bar{q}_a,\quad q_b=\bar{q}_b ,$$

which result in

$$\bar{q}_a=\frac{1}{J_a}\left[\hbar\omega-J_f-\frac{L^2}{2(L^2\bar{q}_b^2/2+W^2)^{1/2}}\right]q_b , \tag{B7a}$$

$$\bar{q}_b=\frac{1}{J_a}\left[\hbar\omega-J_f-\frac{L^2}{2(L^2\bar{q}_a^2/2+W^2)^{1/2}}\right]q_a . \tag{B7b}$$

The solution is $q_a=-\bar{q}_b$, so that $E^a_-=E^b_-$. With $J=J_f-J_a$, Eq. (B5) is essentially the same as Eq. (B3). This solution is correct, independent of the values of J_a,J_f as long as $\hbar\omega-J_f+J_a>0$ and $J_a<0$. This can be proven by inserting

$$\bar{q}=\frac{\sqrt{2}W}{L}(S^2-1)^{1/2}$$

in (B7).

*Present address: Robert Bosch GmbH, D-7000 Stuttgart 1, West Germany.

[1]H. Strunz, Mineral. Tabell. (Leipzig) 5, 283 (1970).

[2]C. A. Beevers and C. M. Schwartz, Z. Kristallogr. 91, 157 (1935).

[3]W. H. Bauer, Acta Crystallogr. 17, 1167 (1964); 17, 1361 (1954).

[4]S. Aslanian, Chr. Balarew, and T. Cikova, Krist. Tech. 7, 525 (1972).

[5]C. Balarew, V. Karaivanova, and S. Aslanian, Krist. Tech. 8, 115 (1973).

[6]H. A. O. Hill and P. Day, *Physical Methods in Advanced Inorganic Chemistry* (Interscience, New York, 1968); R. Janakriaman and G. C. Upreti, Phys. Status Solidi B 47, 679 (1971); R. Chatterjee, Can. J. Phys. 45, 2121 (1967).

[7]W. Kerler and W. Neuwirth, Z. Phys. 167, 176 (1962).

[8]R. Zimmermann and H. Spiering, Phys. Status Solidi B 67, 487 (1975).

[9]R. Ingalls, Phys. Rev. 133, A787 (1963).

[10]H. Spiering, D. L. Nagy, and R. Zimmermann, J. Phys. (Paris) Colloq. 12, C6-1232 (1974).

[11]R. Englman, *The Jahn-Teller Effect in Molecules and Crystals* (Wiley-Interscience, New York, 1972).

[12]V. Ananthanarayanan, Z. Phys. Chem. (Leipzig) 237, 124 (1968).

[13]I. B. Bersuker, Teor. Eksp. Khim 1, 5 (1965).

[14]K. S. Aleksandrov, M. V. Ryzhora, and A. I. Rostuntseva, Kristallografiya 7, 930 (1962) [Sov. Phys.—Crystallogr. 7, 753 (1963)].